Published in : Toxicon (2024), vol. 238, 107569
DOI: https://doi.org/10.1016/j.toxicon.2023.107569
Status : Postprint (Author's version)

BOTHROPS SNAKE VENOM L-AMINO ACID OXIDASES IMPAIR BIOFILM FORMATION OF CLINICALLY RELEVANT BACTERIA

Thales Alves de Melo Fernandes[a], Tássia Rafaella Costa[a], Ralciane de Paula Menezes[b], Meliza Arantes de Souza[b], Carlos Henrique Gomes Martins[b], Nilson Nicolau Junior[c], Fernanda Gobbi Amorim[d], Loïc Quinton[d], Lorena Polloni[a], Samuel Cota Teixeira[e], Eloisa Amália Vieira Ferro[e], Andreimar Martins Soares[f], Veridiana de Melo Rodrigues Ávila[a]

[a] *Laboratory of Biochemistry and Animal Toxins, Institute of Biotechnology, Federal University of Uberlândia, Uberlândia, MG, Brazil*
[b] *Laboratory of Antimicrobial Testing Institute of Biomedical Science, Federal University of Uberlândia, Uberlândia, MG, Brazil*
[c] *Laboratory of Molecular Modeling, Institute of Biotechnology, Federal University of Uberlândia, Uberlândia, MG, Brazil*
[d] *Mass Spectrometry Laboratory, MolSys RU, University of Liège, 4000 Liège, Belgium*
[e] *Laboratory of Immunophysiology of Reproduction, Institute of Biomedical Science, Federal University of Uberlândia, MG, Brazil*
[f] *Laboratory of Biotechnology of Proteins and Bioactive Compounds in the Western Amazon (LABIOPROT), Oswaldo Cruz Foundation, FIOCRUZ Rondônia, Federal University of Rondônia (UNIR), And National Institute of Science and Technology of Epidemiology of the Western Amazon, INCT-EPIAMO, Porto Velho-RO, Brazil*

KEYWORDS

Biofilm ; Bacterial infections ; Antibacterial activity ; Snake venom ; L-amino acid oxidases

ABSTRACT

The present work addressed the abilities of two L-amino acid oxidases isolated from *Bothrops moojeni* (BmooLAAO-I) and *Bothrops jararacussu* (BjussuLAAO-II) snake venoms to control the growth and prevent the biofilm formation of clinically relevant bacterial pathogens. Upon *S. aureus* (ATCC BAA44) and *S. aureus* (clinical isolates), BmooLAAO-I (MIC = 0.12 and 0.24 µg/mL, respectively) and BjussuLAAO-II (MIC = 0.15 µg/mL) showed a potent bacteriostatic effect. Against *E. coli* (ATCC BAA198) and *E. coli* (clinical isolates), BmooLAAO-I (MIC = 15.6 and 62.5 µg/mL, respectively) and BjussuLAAO-II (MIC = 4.88 and 9.76 µg/mL, respectively) presented a lower extent effect. Also, BmooLAAO-I ($MICB_{50}$ = 0.195 µg/mL) and BjussuLAAO-II ($MICB_{50}$ = 0.39 µg/mL) inhibited the biofilm formation of *S. aureus* (clinical isolates) in 88% and 89%, respectively, and in 89% and 53% of *E. coli* (clinical isolates). Moreover, scanning electron microscopy confirmed that the toxins affected bacterial morphology by increasing the roughness of the cell surface and inhibited the biofilm formation. Furthermore, analysis of the tridimensional structures of the toxins showed that the surface-charge distribution presents a remarkable positive region close to the glycosylation motif, which is more pronounced in BmooLAAO-I than BjussuLAAO-II. This region may assist the interaction with bacterial and biofilm surfaces. Collectively, our findings propose that venom-derived antibiofilm agents are promising biotechnological tools which could provide novel strategies for biofilm-associated infections.

Published in : Toxicon (2024), vol. 238, 107569
DOI: https://doi.org/10.1016/j.toxicon.2023.107569
Status : Postprint (Author's version)

GRAPHICAL ABSTRACT

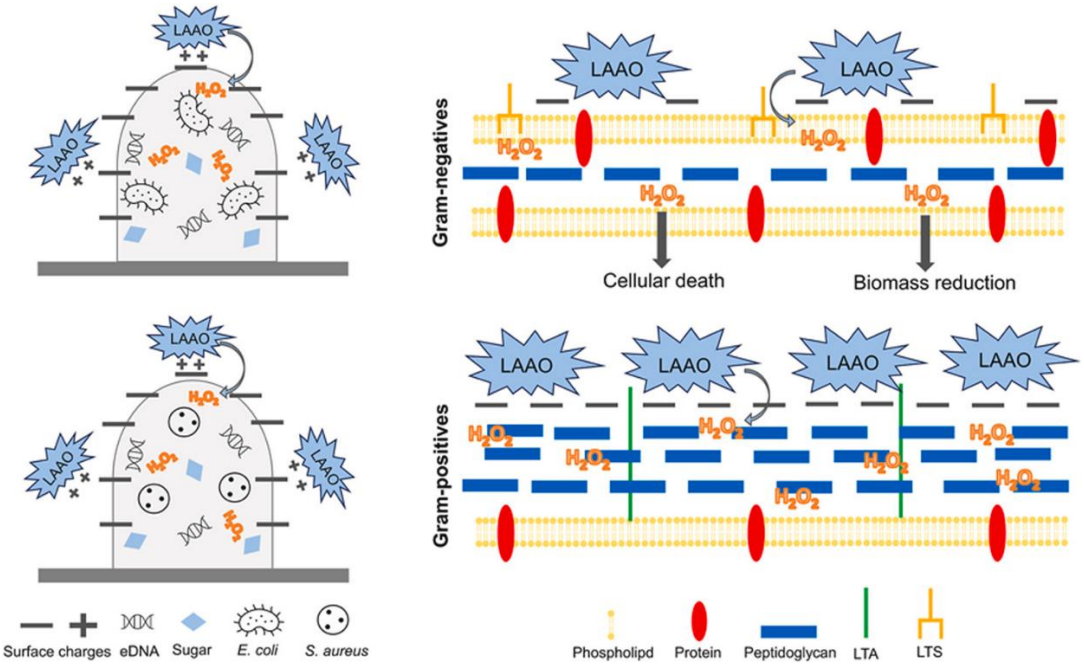

1. Introduction

Biofilm formation contributes to partient morbity and increased mortality rates in bacterial infections (J Del Pozo, 2018). Biofilm corresponds to a sessile bacteria community attached to abiotic or tissue surfaces and sealed on an exopolymeric substance composed of polysaccharides proteins, lipids and extracellular DNA (eDNA) (Singh et al., 2022). Given the importance of biofilm in protecting microorganisms against harsh conditions and contributing to the emergence and dissemination of antibiotic resistance, biofilm formation has been considered as clinically relevant (J Del Pozo, 2018).

Due to the severity of the infections caused by biofilm formation, *Staphylococcus aureus* and *Escherichia coli* have become a serious public health concern (Rabin et al., 2015). *S. aureus* causes a wide range of infections every year due to its ability to invade the bloodstream or internal issues, inducing profound complications in patients' clinical conditions (Cheung et al., 2021; Kwiecinski and Horswill, 2020). In parallel, *E. coli* is the most common cause of bacteria exceeding other leading bacteria-causing pathogens, such as *S. aureus*, and induces severe urinary tract and bloodstream infections (Ballén et al., 2022; Bonten et al., 2021). In this sense, due to the staggering growth of bacterial infections associated with biofilm formation, the search for new and efficient therapeutic agents is necessary.

In this context, snake venoms have been explored as a relevant source of prominent therapeutic biomolecules with a wide spectrum of activities (Oliveira et al., 2022), including L-amino acid oxidases (SV-LAAOs), which possess antibiofilm (Singkham-In et al., 2023), antiprotozoal (de Melo Fernandes et al., 2023) and apoptotic effects (Polloni et al., 2023). SV-LAAOs are flavoenzymes that

Published in : Toxicon (2024), vol. 238, 107569
DOI: https://doi.org/10.1016/j.toxicon.2023.107569
Status : Postprint (Author's version)

catalyze the deamination of an L-amino acid through α-κetoacid and generate hydrogen peroxide (H_2O_2) and ammonia as subproducts (Paloschi et al., 2018). Previously, several studies demonstrated that SV-LAAOs antibacterial action is associated with the production of H2O2, which compromises a range of structures and impairs cell homeostasis (Zhang et al., 2004; Costa et al., 2015; Abdelkafi-Koubaa et al., 2016; Lazo et al., 2017; Oguiura et al., 2023a).

The present work investigated the antibacterial and antibiofilm activities of two L-amino acid oxidases (LAAOs) isolated from *Bothrops moojeni* (BmooLAAO-I) (Stabeli et al., 2007) and *Bothrops jararacussu* (BjussuLAAO-II) (Carone et al., 2017) snake venoms against *S. aureus* and *E. coli* strains. In addition, we correlated the biological effects with the evaluation of the structures of the molecules and suggest possible sites of interaction between the toxins and the bacterial and biofilm surfaces.

2. Material and methods

2.1. CRUDE VENOM AND PURIFICATION OF BMOOLAAO-I AND BJUSSULAAO-II

The crude venoms from *B. moojeni* and *B. jararacussu* were obtained from CETA (Animal Toxin Extraction Center, Ltda - CNPJ: 08.972.260/0001-30, Morungaba SP, Brazil). This serpentarium is certified by the Brazilian Institute of Environment and Renewable Natural Resources (IBAMA) under the registration n° 2/35/1999/000545-1. This work was registered in the National System For The Management Of Genetic Heritage and Associated Traditional Knowledge under the number A2C2534.

The toxins were purified through three chromatographic steps of molecular exclusion in HiPrep Sephacryl S-300 column (GE Healthcare Life Science, PA, USA), hydrophobic interaction in a HiTrap Phenyl-Sepharose 6 Fast Flow (FF) column (GE Healthcare) and affinity to benzamidine in a HiTrap Benzamidine High-Performance (HP) column (GE Healthcare) as previously described (Carone et al., 2017; Barbosa et al., 2021). The protein concentration was determined using Bradford assay (Bradford, 1976). The enzymatic activity was assessed using the spectrophotometric assay with L-Leucine as substrate during the purification and before all the biological experiments, as previously described (Costa et al., 2018). The purified proteins were biochemically evaluated for homogeneity by 12.5% (w/v) SDS-PAGE (Sodium Dodecyl Sulfate-PolyAcrylamide Gel Electrophoresis) in reducing conditions (Laemmli, 1970).

2.2. MASS SPECTROMETRY ANALYSIS

The sequence from the SV-LAAO isolated from *B. jararacussu* snake venom was recently determined by our research group and corresponds to BjussuLAAO-II (Barbosa et al., 2021). In the present study, to confirm the identity of the toxin purified from *B. moojeni* snake venom, the toxin was digested by trypsin and submitted to LC-MS/MS on Acquity M-Class UPLC (Ultra Performance Liquid

Published in : Toxicon (2024), vol. 238, 107569
DOI: https://doi.org/10.1016/j.toxicon.2023.107569
Status : Postprint (Author's version)

Chromatography) (Waters, MA, USA) hyphenated to a Q-Exactive (Thermo Fisher Scientific, IL, USA) in nanoelectrospray positive ion mode, as previously described (Barbosa et al., 2021). The protein identification was performed using Peaks X + Studio v. 10.5 (Ma et al., 2003) against the NCBI (National Center for Biotechnology Information, Bethesda, Maryland, USA) database of "L-amino acid oxidase" from *B. moojeni*. Cysteine carbamidomethylation was set as fixed modification and oxidation as a variable modification and a maximum of 3 missed cleavages of trypsin enzyme. A false discovery rate (FDR) of 0.1%, unique peptide > 1 considering the significant peptides, and only peptides with -10logP > 20 20 were used to detect the proteins from the database search for the SPIDER algorithm (Han et al., 2005).

2.3. BACTERIAL STRAINS

The bacterial strains of *S. aureus* (ATCC BAA44), *E. coli* (ATCC BAA198) and clinical isolates were used to assess the antibacterial and antibiofilm activities. The strains were obtained from ATCC (American Type Culture Collection, MD, USA), while the clinical isolates were kindly supplied by the Clinical Hospital of the School of Medicine of Ribeirao Preto (São Paulo, Brazil) and maintained in the culture collection of the Laboratory of Antimicrobial Testing at the Federal University of Uberlândia (Minas Gerais, Brazil) under cryopreservation at - 80 °C. The strains were cultured in Muller Hinton Agar (DIFCO™, NJ, USA) at 37 °C.

2.4. DETERMINATION OF THE MINIMUM INHIBITORY CONCENTRATION (MIC) AND MINIMUM BACTERICIDAL CONCENTRATION (MBC) OF BMOOLAAO-I AND BJUSSULAAO-II

In order to evaluate the antibacterial activities of BmooLAAO-I and BjussuLAAO-II, the MIC and MBC were determined in triplicate using the microdilution method according to protocols previously described (CLSI Clinical and Laboratory Standards Institute, 2012; Assis et al., 2022). Briefly, 50 µL of BmooLAAO-I or BjussuLAAO-II was added to a 96-well plate containing 50 µL of Muller Hinton broth medium, reaching final concentrations ranging from 0.03 to 312.5 µg/mL. Then, 50 µL per well of the bacterial suspension of *S. aureus*, *E. coli* or the clinical isolates was added reaching the final concentration of 5×10^5 colony-forming units per milliliter (CFU/mL). Bacterial inoculum in the medium without toxin was considered as control group. The plates were incubated at 37 °C for 24 h followed by the addition of 30 µL of 0.02% aqueous resazurin solution to evaluate bacterial growth. MIC values were defined as the lowest concentration able to inhibit the bacterial growth indicated by the color change of resazurin from blue to pink. Before the addition of resazurin, aliquots of 10 µL were transferred from each well to Mueller Hinton agar plates and incubated for 24 h at 37 °C. The MBC was determined by the presence or absence of bacterial growth. In addition, in order to validate the MIC assay, the antibiotic tetracycline was used as control of the experiment in concentrations ranging from 0.01 to 5.9 µg/mL, and the control of the bacterial growth was verified.

Published in : Toxicon (2024), vol. 238, 107569
DOI: https://doi.org/10.1016/j.toxicon.2023.107569
Status : Postprint (Author's version)

2.5. MINIMUM INHIBITORY CONCENTRATION OF BIOFILM FORMATION ($MICB_{50}$) OF BMOOLAAO-I AND BJUSSULAAO-II

The $MICB_{50}$ corresponds to the lowest concentration able to inhibit the biofilm formation by at least 50% (Assis et al., 2022). The $MICB_{50}$ was determined by optical density (OD) measurement at 595-nm of biofilm biomass formed as previously described (Assis et al., 2022). In summary, in 96-well flat-bottom microplates containing Brain Heart Infusion (BHI) broth supplemented with 2% glucose, serial dilutions of the BmooLAAO-I and BjussuLAAO-II (ranging from 0.195 µg/mL to 400) samples were made. From a 24 h culture on BHI agar plates containing 2% of glucose, the inoculum was prepared with turbidity 0.5 on Mac-Farland scale (1×10^5 CFU/mL), measured on a spectrophotometer at 625 nm, and then adjusted to 1×10^6 CFU/mL. The microplates were incubated at 37 °C for 24 h and the contents of the wells were carefully aspirated, and non-adhered cells were removed by gently washing with PBS buffer with pH 7.20. Afterwards, the biofilm formed was fixed with methanol for 15 min, dried at room temperature and stained with a crystal violet solution (0.2%) for 20 min. After removing the crystals and washing the wells with PBS buffer, 33% acetic acid was added for 30 min to solubilize the crystal retained in the biofilm, and the absorbance of the wells was determined in spectrophotometer at 595 nm. In order to determine the number of viable cells in the antibiofilm assay, the cells were gently aspirated and washed with PBS buffer in order to remove non-adhered cells. Next, 200 µL of BHI broth medium with 2% glucose was added to the wells and the microplate was sonicated for 30 min. Subsequently, decimal dilutions were performed (10° to 10^{-7}) and aliquots of 50 µL of each dilution were plated on BHI agar plates and incubated at 37 °C for 24 h. After that, colonies were counted and the results were expressed on a log 10 scale (CFU/mL). The $MICB_{50}$ of BmooLAAO-I and BjussuLAAO-II (ranging from 0.195 to 400 µg/mL) was determined in comparison with the control, incubated with culture medium only. Vancomycin and gentamicin (ranging from 0.01 to 5.9 µg/mL) were used in comparison with the treatments of the toxins. The results were expressed in OD_{595} and viable biofilm cells by counting colony-forming units per milliliter (CFU/mL) in $\log_{10}$ scale. In addition, the percentage (% of biofilm formed) was calculated comparing the absorbance of the toxin treatments with the control (considered as 100% of biofilm formed). Tests were performed in triplicate, and vancomycin and gentamicin (ranging from 0.01 to 5.9 µg/mL) were used in comparison. The inoculum concentration and optimal incubation time for this assay were established by standardizing biofilm formation.

2.6. SCANNING ELECTRON MICROSCOPY ANALYSIS (SEM)

In order to assess the morphological changes induced by the toxin treatments in the cell structure and biofilm, scanning electron microscopy (SEM) was performed according to the methodology previously described (Melo et al., 2017), with minor modifications. The assay was carried out in 24-well plates containing discs of polyvinyl chloride (PVC, diameter 9 mm). Bacterial culture was incubated in absence (control group) or presence of BmooLAAO-I or BjussuLAAO-II at the minimum inhibitory concentrations (MIC) and sub-inhibitory concentrations ($\frac{1}{2}$ MIC). After 24 h of incubation at 37 ° C, the samples were fixed in a solution of 2.5% glutaraldehyde and 2% paraformaldehyde in 0.15 M sodium cacodylate buffer pH 7.0 for 2 h. Then, the samples were post-fixed in 1% osmium

Published in : Toxicon (2024), vol. 238, 107569
DOI: https://doi.org/10.1016/j.toxicon.2023.107569
Status : Postprint (Author's version)

tetroxide solution for 2 h and dehydrated in ethanol at the following concentrations: 30%, 50%, 70%, 90% and 100% with intervals of 20 min each. Subsequently, the samples were subjected to Critical Point Drying (CPD) using liquid carbon dioxide in Leica EM CPD300 (Leica Biosystems, Nuβloch, Germany) coated with gold (20-nm thickness) using Leica EM SCD050 (Leica Biosystems) and analyzed on a scanning electron microscope (Zeiss EVO MA10, Carl Zeiss, Oberkochen, Germany) operating at 20 kV.

2.7. STRUCTURAL EVALUATION OF BMOOLAAO-I AND BJUSSULAAO-II

In order to verify possible sites of interaction between toxins and bacterial surface, the three-dimensional (3D) structures BmooLAAO-I and BjussuLAAO-II were analyzed through the investigation of the electrostatic-surface distribution using the Adaptative Poisson-Boltzmann Solver (APBS) (Baker et al., 2001). Also, we submmited the protein sequences for the prediction of potential sites of antimicrobial regions using AMPA (Torrent et al., 2012). The tertiary structures of BmooLAAO-I and BjussuLAAO-II were predicted using SWISS-MODEL (Waterhouse et al., 2018). Briefly, the protein sequences were submitted to the template search tool and the strucutre of CR-LAAO was selected (PDB: 1FR8). The quality of the predicted models was evaluated using QMEANDisco (Studer et al., 2020), MolProbity (Williams et al., 2018), PROCHEK (Laskowisck et al., 1983), ERRAT (Colovos and Yeates, 1993) and VERIFY3D (Lüthy et al., 1992) in SAVES v.6.0 (https://saves.mbi.ucla.edu/). The protein tertiary visualization and APBS analyses were performed using PyMOL v.2.5 (Schrödinger, Inc., NY, USA). In addition, the sequences of BmooLAAO-I, BjussuLAAO-II and CR-LAAO were submitted to a multiple sequence alignment using the Clustal Omega v. 1.4.2 (Sievers and Higgins, 2018).

2.8. STATISTICAL ANALYSIS

Statistical analyses were performed using GraphPad Prism v.9.0 (GraphPad Software, Inc., CA, USA). Significance differences were analyzed using One-way ANOVA and Tukey's multiple comparisons post-test. The differences were considered significant when $P < 0.05$.

3. Results

3.1. BMOOLAAO-I AND BJUSSULAAO-II WERE SUCCESSFULLY ISOLATED FROM B. MOOJENI AND B. JARARACUSSU VENOMS

The enzymes were successfully purified through the three chromatographic steps of molecular exclusion, hydrophobic interaction and affinity to benzamidine. The purified proteins presented a high homogeneity and migrated as isolated bands of approximately 64 kDa and 60 kDa, corresponding to the molecular mass of BmooLAAO-I and BjussuLAAO-II, respectively. The resulting chromatograms and biochemical characterization are present in the Supplementary Material. The purification process described herein yielded approximately 2.36 mg of BmooLAAO-I and 1.36 mg

Published in : Toxicon (2024), vol. 238, 107569
DOI: https://doi.org/10.1016/j.toxicon.2023.107569
Status : Postprint (Author's version)

BjussuLAAO-II from the crude venom (200 mg), and the toxins displayed enzymatic activity of 4136 and 5205 U/mg/min, respectively.

3.2. MASS SPECTROMETRY EXPERIMENTS CONFIRMED THE IDENTITY OF BMOOLAAO-I FROM B. MOOJENI VENOM

Mass spectrometry analyses resulted in 8896 MS and 25,851 MS^2 scans. After the application of the parameters for scan filtering, the protein has 994 peptide spectrum matches (PSM) and 556 peptides sequences that match the database information. The peptides belong to BmooLAAO-I (National Center for Biotechnology Information (NCBI): AAR31183.1) and present a - 10logP of 603.29, indicating that the protein detected is relatively high in confidence, possesses 95% of coverage with 552 peptides, 1823 *de novo tags* and 102 mass spectra with potential post-translational modifications (PTMs). BmooLAAO-I sequence and the full list of PTMs and mutations are present in the Supplementary Material.

3.3. BMOOLAAO-I AND BJUSSULAAO-II EXHIBITED BACTERIOSTATIC AND BACTERICIDAL EFFECTS UPON GRAM-POSITIVE AND GRAM-NEGATIVE STRAINS

S. aureus ATCC BAA44, *E. coli* ATCC BAA198 and clinical isolates were treated with BmooLAAO-I and BjussuLAAO-II to assess MIC and MBC values. In general, BmooLAAO-I and BjussuLAAO-II exhibited more pronounced bacteriostatic and bactericidal effects against the Gram-positive strains (Table 1). As for the Gram-negatives, BmooLAAO-I and BjussuLAAO-II controlled the bacterial growth and eliminated the microrganisms with a lower extent (Table 1). Regarding tetracycline, the conventional antibiotic inhibited the growth of *S. aureus* and *E. coli* at 0.36 and 0.73 µg/mL.

Table 1. *Minimum Inhibitory Concentrations (MIC) and Minimum Bactericidal Concentrations (MBC) of BmooLAAOO-I and BjussuLAAO-II against Gram-positive and Gram-negative bacterial strains.*

	BmooLAAO-I (µg/mL)		BjussuLAAO-II (µg/mL)	
	MIC	MBC	MIC	MBC
S. aureus **ATCC BAA44**	0.12	0.12	0.15	0.61
S. aureus **Clinical isolates**	0.24	0.24	0.15	0.61
E. coli **ATCC BAA198**	15.6	62.5	4.88	4.88
E. coli **Clinical isolates**	62.5	62.5	9.76	9.76

Published in : Toxicon (2024), vol. 238, 107569
DOI: https://doi.org/10.1016/j.toxicon.2023.107569
Status : Postprint (Author's version)

3.4. BMOOLAAO-I AND BJUSSULAAO-II INHIBITED THE BIOFILM FORMATION OF S. AUREUS AND E. COLI

The antibiofilm activity of BmooLAAO-I and BjussuLAAO-II was assessed through the determination of $MICB_{50}$ and evaluated the amount of biofilm biomass and the number of viable microorganisms. BmooLAAO-I and BjussuLAAO-II demonstrated biofilm inhibitory effects on *S. aureus* (ATCC BAA44), *E. coli* (ATCC BAA198) and the clinical isolates.

BmooLAAO-I induced a significant decline in the biofilm biomass formation of both *S. aureus* ATCC BAA44 and clinical isolates when compared to the control group (Figure 1A and B). Upon *S. aureus* (ATCC BAA44), the $MICB_{50}$ of BmooLAAO-I (0.195 µg/mL) decreased the biomass amount by 91% and reduced the number of microorganisms in -18 $\log_{10}$ CFU/mL units (Figure 1A). Against *S. aureus* (clinical isolates), the $MICB_{50}$ of BmooLAAO-I (0.195 µg/mL) diminished in 88% the biofilm formed and the number of cells in - 14 $\log_{10}$ CFU/mL (Figure 1B).

BjussuLAAO-II also presented prominent effects upon the biofilm biomass development of *S. aureus* ATCC BAA44 and clinical isolates (Figure 1C and D). The $MICB_{50}$ of BjussuLAAO-II (0.195 µg/mL) reduced the *S. aureus* (ATCC BAA44) biofilm biomass in 50% and the number of bacteria in - 6 $\log_{10}$ CFU/mL (Figure 1C). Upon *S. aureus* (clinical isolates), the $MICB_{50}$ BjussuLAAO-II (0.39 µg/mL) diminished in 89% the biomass amount and the number of microorganisms in - 9 $\log_{10}$ CFU/mL (Figure 1D).

In comparison with the vancomycin treatment, BmooLAAO-I and BjussuLAAO-II were more effective in reducing the biofilm formation of *S. aureus* ATCC BAA44 and clinical isolates (Figure 1E and F). The $MICB_{50}$ of vancomycin lowered by 91% the biomass of *S. aureus* (ATCC BAA44) (Figure 1E) and *S. aureus* (clinical isolates) (Figure 1F), corresponding to 0.737 µg/mL and 1.47 µg/mL, respectively. Moreover, the $MICB_{50}$ of vancomycin reduced the number of microorganisms of *S. aureus* (ATCC BAA44) (Figure 1E), at 0.737 µg/mL, and *S. aureus* (clinical isolates) (Figure 1F), at 1.47 µg/mL, in - 15 and - 12 $\log_{10}$ CFU/mL, respectively.

Regarding *E. coli* (ATCC BAA198), BmooLAAO-I presented a lower extent effect (Figure 2A). The $MICB_{50}$ of BmooLAAO-I (100 µg/mL) decreased the biomass by 65% and the number of bacteria in - 7 log 10 CFU/mL (Figure 2A). In parallel, against *E. coli* (clinical isolates), the $MICB_{50}$ of BmooLAAO-I (1.56 µg/mL) reduced by 89% the biofilm formed and the number of microorganisms in - 10 $\log_{10}$ CFU/mL (Figure 2B).

On the other hand, the $MICB_{50}$ of BjussuLAAO-II (1.56 µg/mL) diminished in 60% and 54% the biomass of *E. coli* (ATCC BAA198) (Figure 2C) and *E. coli* (clinical isolates) (Figure 2D), respectively. Moreover, at this concentration, BjussuLAAO-II reduced the number of cells in - 6 and - 7 log 10 CFU/mL of *E. coli* (ATCC BAA198) (Figure 2C) and *E. coli* (clinical isolates) (Figure 2D), respectively.

Compared to gentamicin, BmooLAAO-I and BjussuLAAO-II were more effective in inhibiting the biofilm biomass formation of *E. coli* ATCC BAA198 and the clinical isolates (Figure 1E and F). Gentamicin only at the highest concentration, $MICB_{50}$ of 5.9 µg/mL, reduced in 70% and 62% the biofilm formed of *E. coli* (ATCC BAA198) (Figure 2E) and *E. coli* (clinical isolates) (Figure 2F),

Published in : Toxicon (2024), vol. 238, 107569
DOI: https://doi.org/10.1016/j.toxicon.2023.107569
Status : Postprint (Author's version)

respectively. Also, the $MICB_{50}$ of gentamicin lowered in - 9 and -7 log 1- CFU/mL the number of *E. coli* (ATCC BAA198) (Figure 2E) and *E. coli* (clinical isolates) (Figure 2F) cells, respectively.

Figure 1. *Antibiofilm activity of BmooLAAO-I, BjussuLAAO-II and vancomycin against S. aureus ATCC BAA44 and clinical isolates. Representative graphs of S. aureus (ATCC BAA44) after treatment with (A) BmooLAAO-I, (C) BjussuLAAO-II and (E) Vancomycin. Effects of (B) BmooLAAO-I, (D) BjussuLAAO-II and (F) Vancomycin upon S. aureus (clinical isolates). The microorganisms were treated with two-fold serial dilutions of BmooLAAO-I or BjussuLAAO-II (ranging from 0.195 to 400 μg/mL) for 24 h. The bacteria were incubated with vancomycin (ranging from 0.01 to 5.9 μg/mL) for comparison with the toxin treatment. The control group corresponds to the microorganisms incubated with culture medium only. The results were expressed as optical density (OD) (bars) measured at 595 nm and log_{10} CFU/mL (scatter plot). The labeled bars correspond to the $MICB_{50}$ calculated by the OD values. The data are shown as means ± standard deviation from experiments performed in triplicate. Significant differences between groups were evaluated by One-Way ANOVA and Tukey's multiple comparison post-test. *Comparison between all treatments and control group (**** P < 0.0001, *** P < 0.001, ** P < 0.01, * P < 0.05).*

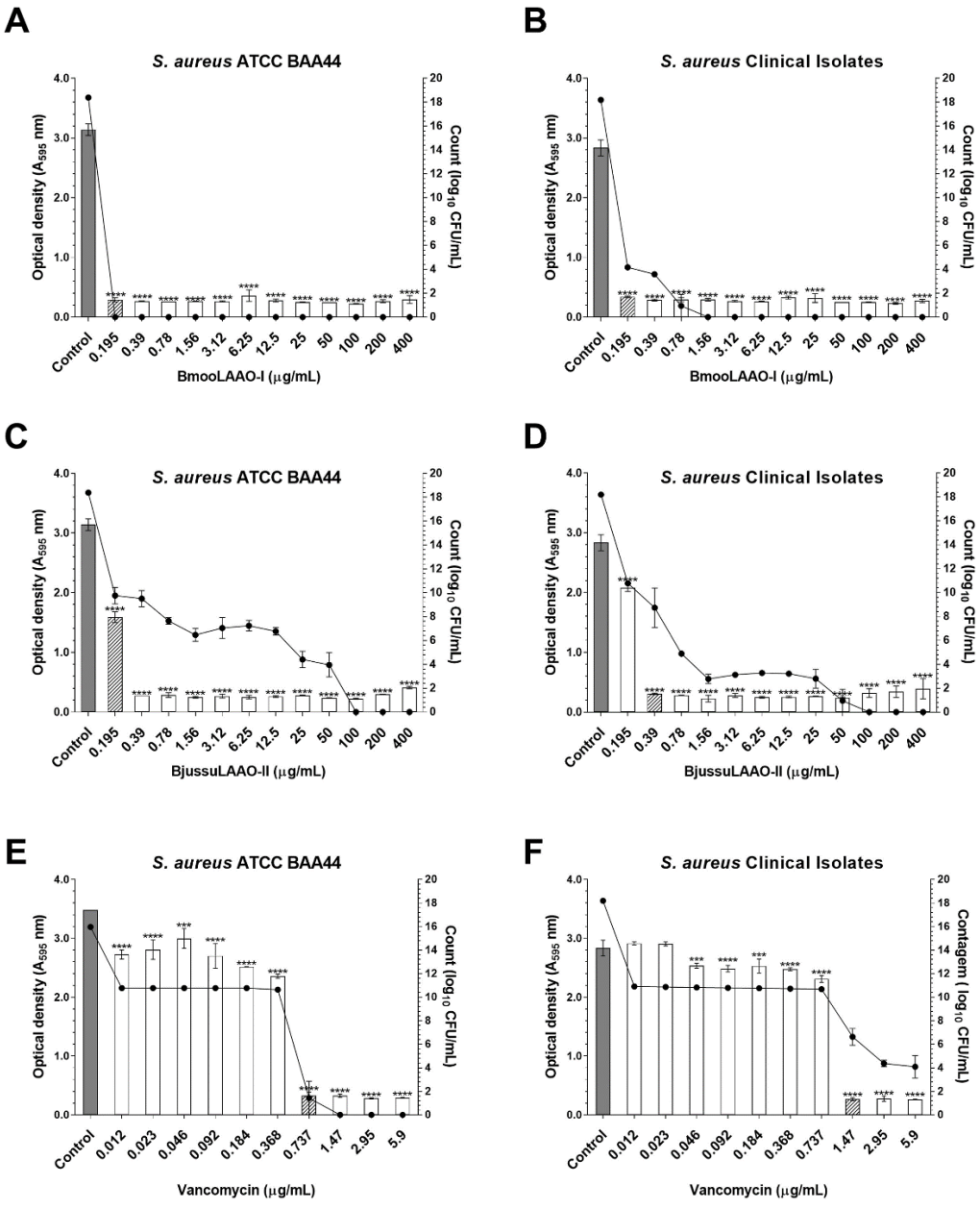

Published in : Toxicon (2024), vol. 238, 107569
DOI: https://doi.org/10.1016/j.toxicon.2023.107569
Status : Postprint (Author's version)

Figure 2**. Antibiofilm activity of BmooLAAO-I, BjussuLAAO-II and gentamicin against E. coli ATCC BAA198 and clinical isolates. Effects of different concentrations of (A) BmooLAAO-I, (C) BjussuLAAO-II and (E) Gentamicin in E. coli (ATCC BAA198). Representative graphs of E. coli (clinical isolates) after treatment with (B) BmooLAAO-I, (D) BjussuLAAO-II and (F) Gentamicin. The microorganisms were treated with two-fold serial dilutions of BmooLAAO-I or BjussuLAAO-II (ranging from 0.195 to 400 μg/mL) for 24 h. The bacteria were incubated with gentamicin (ranging from 0.01 to 5.9 μg/mL) for comparison with the toxin treatment. The control group corresponds to the microorganisms incubated with culture medium only. The results were expressed as optical density (OD) (bars) measured at 595 nm and $\log_{10}$ CFU/mL (scatter plot). The labeled bars correspond to the $MICB_{50}$ calculated by the OD values. The data are shown as means ± standard deviation from experiments performed in triplicate. Significant differences between groups were evaluated by One-Way ANOVA and Tukey's multiple comparison post-tests. *Comparison between all treatments and control group (* P < 0.0001, *** P < 0.001, ** P < 0.01, * P < 0.05).*

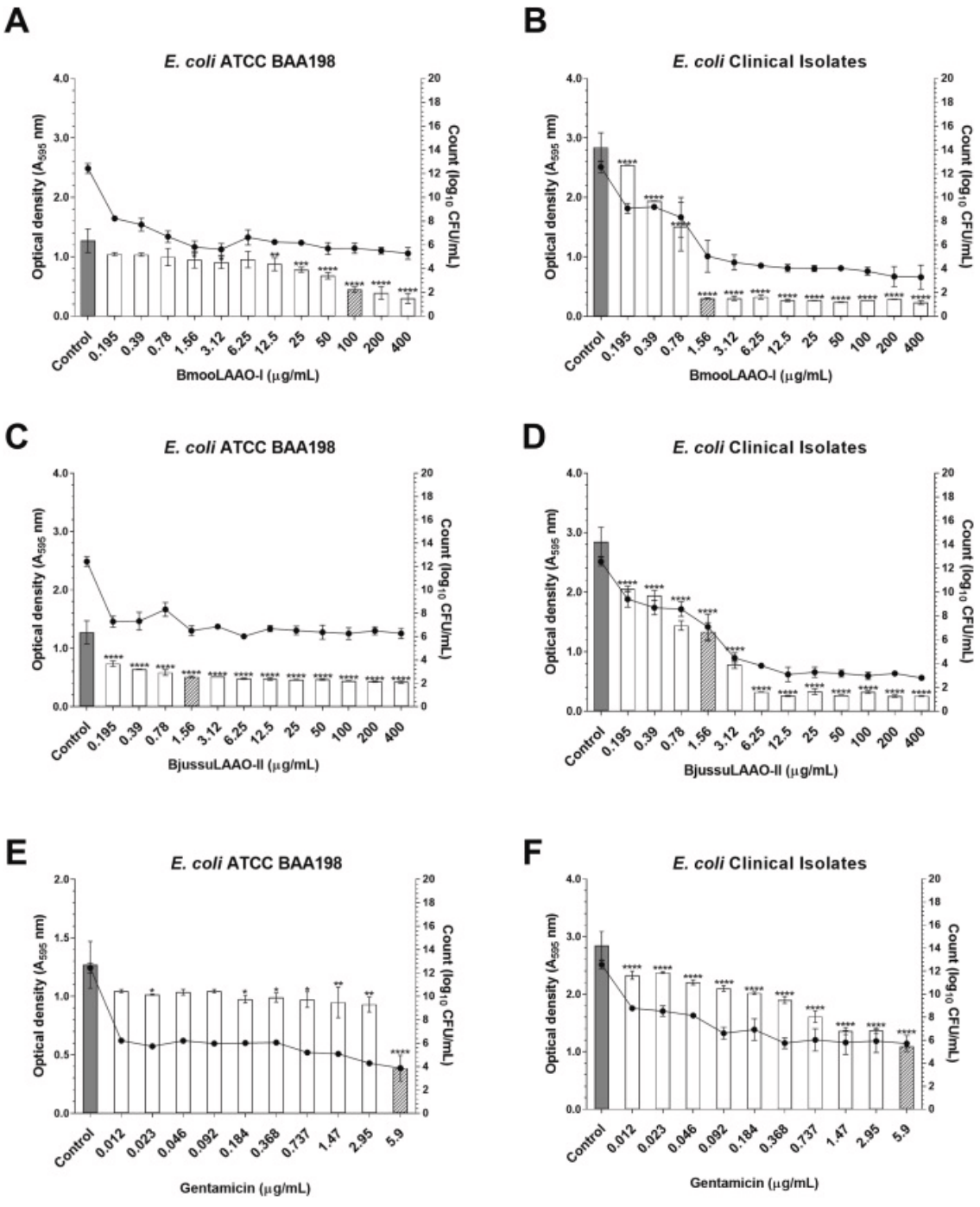

Published in : Toxicon (2024), vol. 238, 107569
DOI: https://doi.org/10.1016/j.toxicon.2023.107569
Status : Postprint (Author's version)

3.5. BMOOLAAO-I AND BJUSSULAAO-II ALTERED THE BIOFILM MATRIX PRODUCTION AND THE BACTERIAL MORPHOLOGY

MIC treatments of BmooLAAO-I and BjussuLAAO-II altered the bacterial cluster architecture and matrix production was extremely poor when compared to the control group of *S. aureus* ATCC BAA44 (Figure 3A (C) and 3 A(G), respectively). Moreover, against *S. aureus* (clinical isolates), MIC of BmooLAAO-I and BjussuLAAO-II altered the number of bacterial clusters deficient in matrix production and the cell morphology (Figure 3A(D) and 3 A(H), respectively). In contrast, at the concentration of $\frac{1}{2}$ MIC of BmooLAAO-I and BjussuLAAO-II, the cells and biofilm morphology of *S. aureus* ATCC BAA44 and the clinical isolates were similar to the control group (Figure 3A(I-J)).

In relation to *E. coli* (ATCC BAA198), MIC of BmooLAAO-I and BjussuLAAO-II resulted in a decrease in biofilm thickness and an increase in the roughness of cell surface (Figure 3B(C) and 3 B(G), respectively). At the $\frac{1}{2}$ MIC concentration, BmooLAAO-I and BjussuLAAO-II induced changes in morphology of *E. coli* ATCC BAA198 biofilm (Figure 3B (E) and 3 B(I), respectively) Upon *E. coli* (clinical isolates), MIC of BmooLAAO-I and BjussuLAAO-II affected both biofilm matrix and the cell surface (Figure 3B(D) and 3 B(H), respectively). Alternatively, the $\frac{1}{2}$ MIC of BmooLAAO-I and BjussuLAAO-II induced changes in cell morphology without changing the biofilm matrix (Figure 3B(F) and 3 B(J), respectively).

Figure 3*. Scanning Electron Microscopy (SEM) of (A) S. aureus and (B) E. coli. Representative images of S. aureus ATCC BAA44, E. coli (ATCC BAA198), S. aureus (clinical isolates) and E. coli (clinical isolates) treated for 24 h with MIC or $\frac{1}{2}$ MIC of BmooLAAO-I and BjussuLAAO-II. White arrows indicate: (a) Extracellular Polymeric Substance (EPS); (b) cellular integrity preserved; (c) aqueous channels; (d) roughness; (e) cellular division. The captions were obtained with magnification of 40,000 × at 20 kV. Scale bar: 1 μm.*

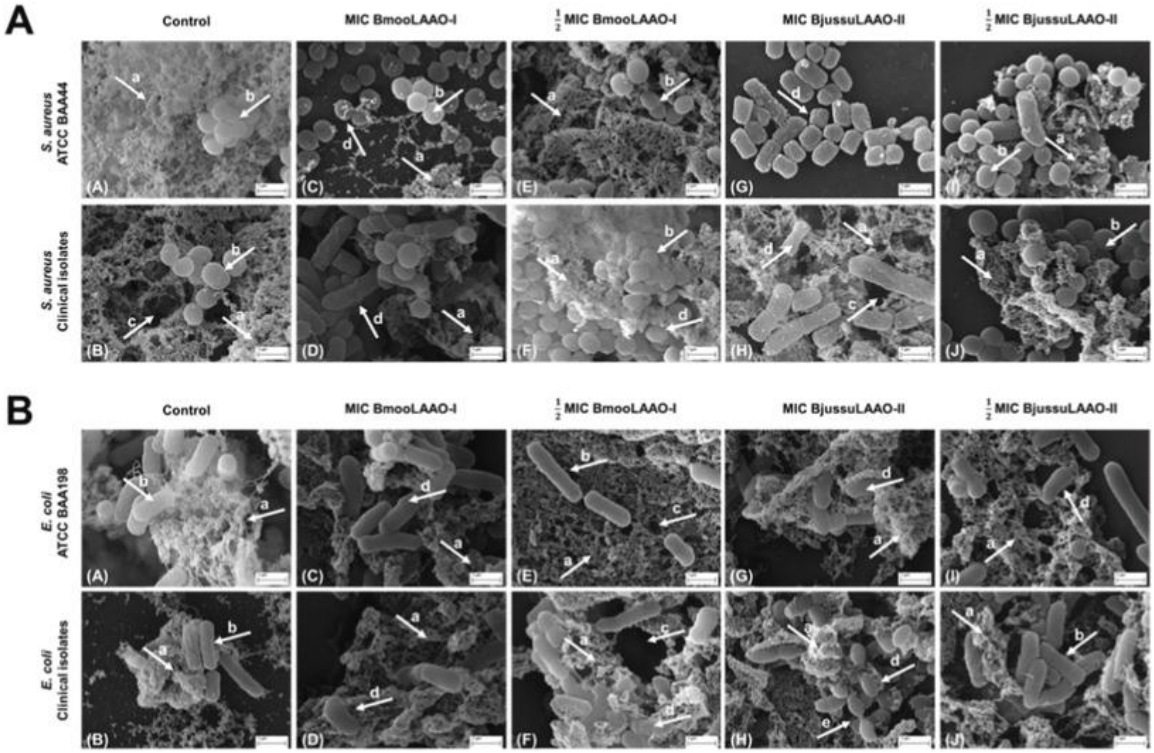

Published in : Toxicon (2024), vol. 238, 107569
DOI: https://doi.org/10.1016/j.toxicon.2023.107569
Status : Postprint (Author's version)

3.6. BMOOLAAO-I AND BJUSSULAAO-II STRUCTURES SHED LIGHTS TO POSSIBLE SITES OF INTERACTION WITH THE BACTERIAL SURFACE

In order to correlate the structures of both SV-LAAOs with their antibacterial and antibiofilm effects, the predicted models of BmooLAAO-I and BjussuLAAO-II were evaluated. The models of BmooLAAO-I and BjussuLAAO-II presented an excellent stereochemical quality. The QMEANDisCo validated the models with quality of 0.85 and 0.79, respectively. The ERRAT indicated a general quality of 90.5 and 95.0, respectively. The PROCHEK and MolProbity pointed out to a good distribution of the atoms and torsional angles in the Ramachandran plot. MolProbity showed that 99.8% and 99.6% of the residues occupied allowed regions for BmooLAAO-I and BjussuLAAO-II, respectively. The stereochemical quality assessment results are present in the Supplementary Material.

The predicted proteins are organized in a homodimeric structure composed of chains A and B in an asymmetric configuration. Each monomer conserved the three domains of SV-LAAOs: FAD-binding domain, substrate-binding domain and helical domain (Figure 4A and B). The superposition between all atoms and Cα revealed an 0RMSD of 0.105 and 0.078 Å, respectively, indicating that the proteins possess a high structural pattern similarity, which correlates with the high degree of identity in the primary structure. Interestingly, the surface-charge distribution exhibited a remarkable positive site close to the glycosylation motif involving residues from the substrate-binding domain and FADbinding domain, which is more pronounced in BmooLAAO-I than BjussuLAAO-II (Figure 5A and B).

Furthermore, the multiple sequence alignment (MSA) analysis showed that BmooLAAO-I and BjussuLAAO-II present a high identity in the primary structure (88%). The template of CR-LAAO shares an identity with BmooLAAO-I of 81% and BjussuLAAO-II of 83%. Also, the proteins conserved the consensus glycosylation sites of Asn 172 and Asn 361. The MSA is present in the Supplementary Material.

Supporting the antibacterial and antibiofilm effects with the evaluation of the protein structures, we submitted the sequences for the prediction of antimicrobial regions using AMPA. We observed that both BmooLAAO-I and BjussuLAAO-II possess potential antimicrobial regions distributed along their primary structure encompassing the substrate and FAD-binding domains. The AMPA plot results can be visualized in the Supplementary Material.

Published in : Toxicon (2024), vol. 238, 107569
DOI: https://doi.org/10.1016/j.toxicon.2023.107569
Status : Postprint (Author's version)

Figure 4. *BmooLAAO-I and BjussuLAAO-II predicted models. Cartoon representation of the dimer from (A) BmooLAAO-I and (B) BjussuLAAO-II. Chain A is colored in yellow and chain B in cyan. Structural domains of (C) BmooLAAO-I and (D) BjussuLAAO-II. The substrate-binding domain, the FAD-binding domain and the helical domain are labeled in green, blue and red, respectively. The FAD cofactor is represented in balls and sticks. (For interpretation of the references to color in this figure legend, the reader is referred to the Web version of this article.)*

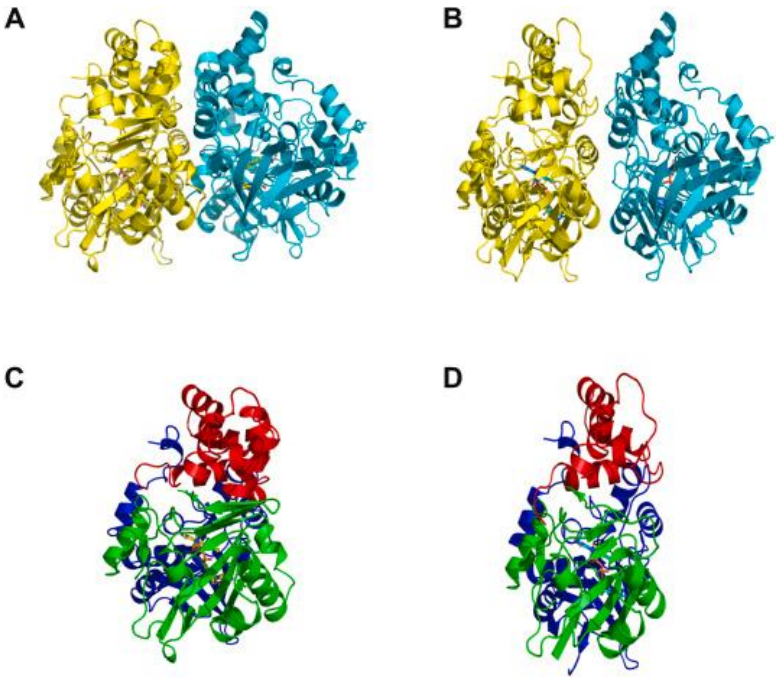

Figure 5. *Surface charge distribution in BmooLAAO-I and BjussuLAAO-II. The white, blue and red colors indicate neutral, positive and negative charges, respectively, in (A) BmooLAAO-I and (B) BjussuLAAO-II. The panel on the left corresponds to the front view and the right panel represents the bottom view. (For interpretation of the references to color in this figure legend, the reader is referred to the Web version of this article.)*

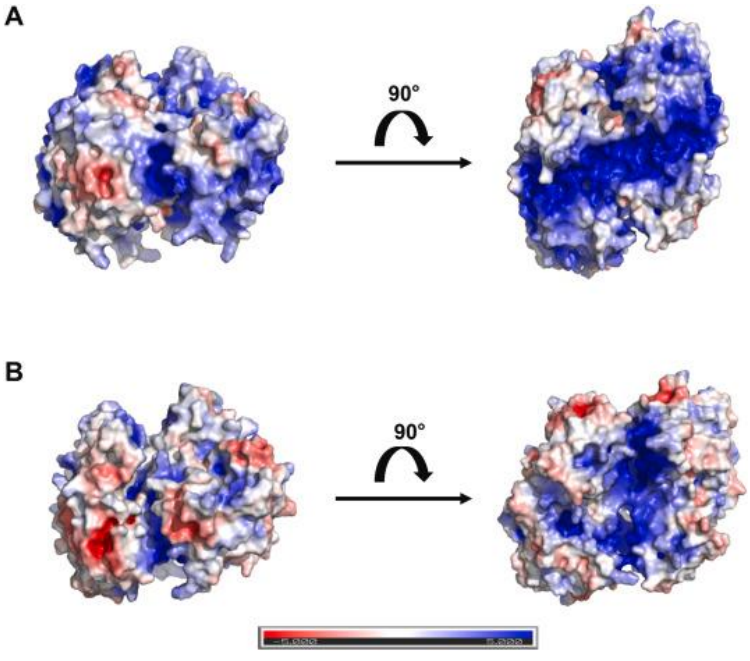

Published in : Toxicon (2024), vol. 238, 107569
DOI: https://doi.org/10.1016/j.toxicon.2023.107569
Status : Postprint (Author's version)

4. Discussion

Biofilm formation accounts for up to 80% of all bacterial infections and is considered as one of the main causes of high mortality (Singh et al., 2022). *S. aureus* and *E. coli* bacteria species are among the main pathogens associated with biofilm formation, causing bone, joint, lung, urinary and bloodstream infections (Cheung et al., 2021; Kwiecinski and Horswill, 2020; Ballén et al., 2022; Bonten et al., 2021). Due to the staggering growth of bacterial infections associated with biofilm formation, there is an urgent need for new and effective therapeutic agents. In this context, the present work evaluated the antibacterial and antibiofilm activities of two LAAOs isolated from *B. moojeni* and *B. jararacussu* snake venoms against *S. aureus* and *E. coli* and pointed out to potential interactions sites between the structure of both toxins on the bacterial and biofilm surface.

BmooLAAO-I and BjussuLAAO-II were isolated through three chromatographic steps of molecular exclusion, hydrophobic interaction and affinity to benzamidine. Although we reproduced the purification methodology described for the purification of BmooLAAO-II (Barbosa et al., 2021), we obtained the BmooLAAO-I isoform, which was identified by sequence determination through mass spectrometry analysis. BmooLAAO-I and BjussuLAAO-II were previously biochemically characterized and possess a preference for hydrophobic amino acids, such as L-Phenylalanine and L-Leucine, wide temperature stability (ranging from 25 to 75 °C) and optimum pH around 7.0. Additionally, Zn^{2+}, Al^{3+}, Cu^{2+}, and Ni^{2+} ions negatively modulated the enzymatic activity of both proteins (Costa et al., 2018). Also, these toxins display relevant biological activities, such as antibacterial (Stábeli et al., 2007; Carone et al., 2017), antiprotozoal (de Melo Fernandes et al., 2023; Stábeli et al., 2007; Carone et al., 2017; Barbosa et al., 2021), antitumoral (Burin et al., 2020; Machado et al., 2018, 2019a, 2019b) and immunomodulatory effects (Pereira-Crott et al., 2020). Most of the biological effects of BmooLAAO-I and BjussuLAAO-II involved the production of hydrogen peroxide (de Melo Fernandes et al., 2023; Stábeli et al., 2007; Barbosa et al., 2021; Machado et al., 2018, 2019b).

BmooLAAO-I and BjussuLAAO-II exhibited bactericidal and bacteriostatic effects against *S. aureus* (ATCC BAA44), *E. coli* (ATCC BA198) and clinical isolates. Interestingly, the toxins presented a greater effect against Gram-positive bacteria than Gram-negative. Corroborating with these results, different SV-LAAOs also presented a bacteriostatic preference effect upon Gram-positives, such as BsLAAO (Vargas Muñoz et al., 2014), CdcLAAO (Toyama et al., 2006) and MipLAAO (Rey-Suárez et al., 2018). In addition to the effect on planktonic bacteria, BmooLAAO-I and BjussuLAAO-II inhibited the biofilm formation of *S. aureus* and *E. coli* and caused alterations in the microrganism morphology and biofilm architecture. Some studies demonstrated that LAAOs isolated from different organisms exhibited the antibiofilm activity through oxidative stress (Singkham-In et al., 2023; Derby et al., 2018; Tong et al., 2008). LAAO isolated from the inking sea hare *Apkysis californica* inhibited the biofilm formation of *Pseudomonas aeruginosa* through the oxidative damage of intracellular and extracellular eDNA (Derby et al., 2018). Moreover, SO-LAAO from *Streptococcus oligofermentans*, an oral streptococcus, generated H_2O_2 and suppressed the biofilm formation of *S. mutans* (Tong et al., 2008). Recently, Singkham et al. (2023) demonstrated that the antibiofilm activities of OH-LAAO from *Ophiophagus hannah* snake against *P. aeruginosa* were mediated by H_2O_2 downregulation of genes

Published in : Toxicon (2024), vol. 238, 107569
DOI: https://doi.org/10.1016/j.toxicon.2023.107569
Status : Postprint (Author's version)

involved in biofilm synthesis (Singkham-In et al., 2023). Although we have not explored the role of the hydrogen peroxide in the control of biofilm formation, those strong evidences points to the involvement of H_2O_2 in the antibiofilm effects of LAAOs.

The antibacterial activity of numerous SV-LAAOs has been extensively investigated and is correlated to the hydrogen peroxide generated during the catalytic cycle (Kasai et al., 2021). In bacteria, the major antioxidant agents of reactive oxygen species (ROS) are superoxide dismutase (SOD) and catalase (CAT) (Vatansever et al., 2013). The H_2O_2 damages structural components of bacteria, such as proteins, DNA, lipids, and the cell wall, causing oxidative stress and cellular death (Vatansever et al., 2013). Moreover, the SV-LAAOs were shown to be~able to bind the microorganism surfaces and generate high concentrations of localized hydrogen peroxide promoting oxidative stress (Abdelkafi-Koubaa et al., 2016; Lee et al., 2011). That ability of attachment on cell surfaces was pointed out to be mediated by the glycan motif, composed often by N-acetylglucosamine, fucose, mannose, galactose and sialic acid residues (Ullah, 2020). In molecular simulation with membrane surfaces, it was verified that those proteins interact via the residues of the FAD-binding loop and the N-glycosylation motif (Ullah, 2020). The glycan moiety is near the O_2 entrance and H_2O_2 exit tunnel and has been connected with the high concentration of hydrogen peroxide generated in the cell surface through the attachment of different SV-LAAOs (Ullah, 2020).

The bacteria cell walls present a special role in the microorganism life, protecting against hostile environment, shaping the cell format, providing ligands for adherence in host cells and structures of virulence (Nourbakhsh et al., 2022). Gram-positive and Gram-negative bacteria possess a negatively charged surface character (Fischetti, 2019). Also, the microrganisms secrete polysaccharides, eDNA and peptides during the adhesion and maturation stages of biofilm formation (Ruhal and Kataria, 2021). These molecules are necessary to maintain the architecture and are also important in sequestring positive-charge antibiotics, due to their electrotatic nature (Wilton et al., 2015).

Correlating these important characteristics of the cell wall and the biofilm compostion with the binding ability mediated by the glycan motif of the SV-LAAOs and oxidative stress damage, the differences in the effect of BmooLAAO-I and BjussuLAAO-II against Gram-positive and Gram-negative planktonic cells and biofilm can be clarified. In this context, BmooLAAO-I and BjussuLAAO-II possess different compositions and numbers of N-glycosylation sites (Costa et al., 2018). BmooLAAO-I presents three glycosylation sites and BjussuLAAO-II has two sites. Moreover, BmooLAAO-I possesses a greater positive-charged area encompassing the substrate-binding domain and FAD-binding domain than BjussuLAAO-II close to the N-glycosylation site. This more pronounced positive electrostatic surface was also observed in bordonein-L and was suggested to be fundamental in the biological role of this enzyme (Wiezel et al., 2019). In this sense, we believe that the interaction between the carbohydrate residues and stabilizing electrostatics forces could impact the binding ability of BmooLAAO-I and BjussuLAAO-II to the bacterial and biofilm surfaces of Gram-positive and Gram-negative bacteria, contributing to the oxidative stress promoted by the generation of high concentrations of localized hydrogen peroxide, as pointed out previously (Abdelkafi-Koubaa et al., 2016; Lee et al., 2011).

Published in : Toxicon (2024), vol. 238, 107569
DOI: https://doi.org/10.1016/j.toxicon.2023.107569
Status : Postprint (Author's version)

The use of SV-LAAOs for the treatment of biofilm-associated bacterial infections must take into account their selectivity and toxicological effects. In this sense, an improvement of our work would be addressing the pharmacological properties of BmooLAAO-I and BjussuLAAO-II, investigating their antibiofilm potential and cytoxicity on the host cells. Recently, Abdelkafi-Koubaa et al. (2021), explored the potential use CC-LAAO, an L-amino acid oxidase isolated from *Cerastes*, as an anti-glioblastoma drug through the investigation of the pharmacological effects (Abdelkafi-Koubaa et al., 2021). Using blood parameters and histopathological examination, CC-LAAO at low doses (1 and 2.5 µg/mL) did not induce significant toxicity on vital organs, and may be safe for the development of anti-glioblastoma agents.

Furthermore, the identification of small fragments that reproduce the antibacterial effect can be a promising pathway. In this context, in comparison with conventional antibiotics, antimicrobial proteins and peptides (AMPs) efficiently inhibit pathogenic microorganisms targeting the cell membranes and do not induce the generation of resistant mutant microorganisms after sequential exposure (Oguiura et al., 2023b). There are numerous reports of AMPs corresponding to peptide fragments of snake toxins able to inhibit the growth and kill pathogenic microorganisms (Costa et al., 2008; Santos-Filho et al., 2015; Almeida et al., 2021). Among them, fragments of BmLAO isolated from *B. mattogrosensis* presented antimicrobial activities against Gram-negative and Gram-positive pathogens (Peña-Carrillo et al., 2021). Several AMPs that target bacteria are cationic and may interact with the anionic lipid components that are exposed on the bacterial membrane (Okubo et al., 2012). In this sense, one interesting approach would be the generation of small peptides from the positive charged surface of BmooLAAO-I and BjussuLAAO-II and the investigation of their antibacterial and antibiofilm potential.

5. Conclusion

In summary, our present work revealed important antibacterial and antibiofilm properties of two L-amino acid oxidases (LAAOs) isolated from *B. moojeni* (BmooLAAO-I) and *B. jararacussu* (BjussuLAAO-II) snake venoms against *S. aureus* and *E. coli*. We showed that the isolated toxins presented a strong bacteriostatic and bactericidal action against planktonic microorganisms and inhibit biofilm formation. We correlated the disparity of effect against the Gram-positive and Gram-negative with structural characteristics of the protein and bacterial compositional patterns. The results pointed out to the potential biotechnological use of natural compounds isolated from snake venoms for the development of new and more effective agents against bacterial infections associated with biofilm formation.

Published in : Toxicon (2024), vol. 238, 107569
DOI: https://doi.org/10.1016/j.toxicon.2023.107569
Status : Postprint (Author's version)

FUNDING

The authors gratefully acknowledge the financial support by Universidade Federal de Uberlândia (UFU), Conselho Nacional de Desenvolvimento Científico e Tecnológico (CNPq), Fundação de Amparo a Pesquisa do Estado de Minas Gerais (FAPEMIG) (grant number CBB - APQ-01401-17), Coordenação de Aperfeiçoamento de Pessoal de Nível Superior - Brasil (CAPES) and the National Institute of Science and Technology in Theranostics and Nanobiotechnology INCT-TeraNano- CNPq/CAPES/FAPEMIG (grant number CNPq-465,669/2014-0). The Q-Exactive mass spectrometer was funded by ERDF and the Walloon Region grant and Peaks X+ version Studio 10.5 software was funded by ERDF's grant: BIOMED HUB Technology Support (grant number 2.2.1/ 996).

CREDIT AUTHORSHIP CONTRIBUTION STATEMENT

Thales Alves de Melo Fernandes: Conceptualization, Data curation, Investigation, Validation, Visualization, Writing - original draft, Writing - review & editing. Tássia Rafaella Costa: Conceptualization, Data curation, Formal analysis, Investigation, Supervision, Validation, Visualization. Ralciane de Paula Menezes: Data curation, Formal analysis, Investigation, Validation, Visualization, Writing - review & editing. Meliza Arantes de Souza: Data curation, Formal analysis, Investigation, Visualization, Writing - original draft. Carlos Henrique Gomes Martins: Conceptualization, Formal analysis, Resources, Writing - original draft, Writing - review & editing. Nilson Nicolau Junior: Conceptualization, Data curation, Formal analysis, Investigation, Validation, Writing - original draft, Writing - review & editing. Fernanda Gobbi Amorim: Data curation, Formal analysis, Investigation, Validation, Visualization, Writing - original draft, Writing - review & editing. Loïc Quinton: Data curation, Formal analysis, Investigation, Validation, Visualization, Writing - original draft. Lorena Polloni: Formal analysis, Investigation, Visualization, Writing - original draft, Writing - review & editing. Samuel Cota Teixeira: Data curation, Formal analysis, Investigation, Validation, Visualization, Writing - original draft, Writing - review & editing. Eloisa Amália Vieira Ferro: Resources, Writing - original draft, Writing - review & editing. Andreimar Martins Soares: Resources, Writing - original draft, Writing - review & editing. Veridiana de Melo Rodrigues Ávila: Conceptualization, Data curation, Resources, Supervision, Validation, Visualization, Writing - original draft, Writing - review & editing.

ACKNOWLEDGMENTS

The authors thank the GIGA-Proteomics platform (ERDF funding) for the technical support, specially Maximilien Fléron and Dominique Baiwir from the GIGA-Proteomics Facility of the University of Liege for the use of the mass spectrometer instruments. Moreover, the authors acknowledge the Scanning Electron Microscopy Multi-user Laboratory (LAMEV) from the Chemical Engineering College of Uberlandia Federal University, particularly technician Rafael Ramos Heilbuth for the utilization of the microscope and obtaining of SEM images. This article has been edited by the proofreader and professional ESL/EFL teacher Abilio Antonio Borghi.

APPENDIX A. SUPPLEMENTARY DATA

Supplementary data to this article can be found online at

https://doi.org/10.1016/j.toxicon.2023.107569

Published in : Toxicon (2024), vol. 238, 107569
DOI: https://doi.org/10.1016/j.toxicon.2023.107569
Status : Postprint (Author's version)

References

Abdelkafi-Koubaa, Z., Aissa, I., Morjen, M., Kharrat, N., El Ayeb, M., Gargouri, Y., Srairi-Abid, N., Marrakchi, N., 2016. Interaction of a snake venom L-amino acid oxidase with different cell types membrane. Int. J. Biol. Macromol. 82, 757–764. https://doi.org/10.1016/j.ijbiomac.2015.09.065.

Abdelkafi-Koubaa, Z., Elbini-Dhouib, I., Souid, S., Jebali, J., Doghri, R., Srairi-Abid, N., Essafi-Benkhadir, K., Micheau, O., Marrakchi, N., 2021. Pharmacological investigation of CC-LAAO, an L-amino acid oxidase from *Cerastes cerastes* snake venom. Toxins 13 (12), 904. https://doi.org/10.3390/toxins13120904.

Almeida, J.R., Mendes, B., Lancellotti, M., Franchi Jr., G.C., Passos, Ó., Ramos, M.J., Fernandes, P.A., Alves, C., Vale, N., Gomes, P., da Silva, S.L., 2021. Lessons from a single amino acid substitution: anticancer and antibacterial properties of two phospholipase A_2-derived peptides. Curr. Issues Mol. Biol. 44 (1), 46–62. https://doi.org/10.3390/cimb44010004.

Assis, L.R., Theodoro, R.D.S., Costa, M.B.S., Nascentes, J.A.S., Rocha, M.D.D., Bessa, M.A.S., Menezes, R.P., Dilarri, G., Hypolito, G.B., Santos, V.R.D., Duque, C., Ferreira, H., Martins, C.H.G., Regasini, L.O., 2022. Antibacterial activity of isobavachalcone (IBC) is associated with membrane disruption. Membranes 12 (3), 269. https://doi.org/10.3390/membranes12030269.

Baker, N.A., Sept, D., Joseph, S., Holst, M.J., McCammon, J.A., 2001. Electrostatics of nanosystems: application to microtubules and the ribosome. Proc. Natl. Acad. Sci. U. S. A. 98 (18), 10037–10041. https://doi.org/10.1073/pnas.181342398.

Ballén, V., Cepas, V., Ratia, C., Gabasa, Y., Soto, S.M., 2022. Clinical *Escherichia coli*: from biofilm formation to new antibiofilm strategies. Microorganisms 10 (6), 1103. https://doi.org/10.3390/microorganisms10061103.

Barbosa, L.G., Costa, T.R., Borges, I.P., Costa, M.S., Carneiro, A.C., Borges, B.C., Silva, M.J.B., Amorim, F.G., Quinton, L., Yoneyama, K.A.G., de Melo Rodrigues, V., Sampaio, S.V., Rodrigues, R.S., 2021. A comparative study on the leishmanicidal activity of the L-amino acid oxidases BjussuLAAO-II and BmooLAAO-II isolated from Brazilian *Bothrops* snake venoms. Int. J. Biol. Macromol. 167, 267–278. https://doi.org/10.1016/j.ijbiomac.2020.11.146.

Bonten, M., Johnson, J.R., van den Biggelaar, A.H.J., Georgalis, L., Geurtsen, J., de Palacios, P.I., Gravenstein, S., Verstraeten, T., Hermans, P., Poolman, J.T., 2021. Epidemiology of *Escherichia coli* bacteremia: a systematic literature review. Clin. Infect. Dis. 72 (7), 1211–1219. https://doi.org/10.1093/cid/ciaa210.

Bradford, M.M., 1976. A rapid and sensitive method for the quantitation of microgram quantities of protein utilizing the principle of protein-dye binding. Anal. Biochem. 72, 248–254. https://doi.org/10.1006/abio.1976.9999.

Burin, S.M., Cacemiro, M.D.C., Cominal, J.G., Grandis, R.A., Machado, A.R.T., Donaires, F.S., Cintra, A.C.O., Ambrosio, L., Antunes, L.M.G., Sampaio, S.V., de Castro, F.A., 2020. *Bothrops moojeni* L-amino

acid oxidase induces apoptosis and epigenetic modulation on Bcr-Abl+ cells. J. Venom. Anim. Toxins Incl. Trop. Dis. 26, e20200123 https://doi.org/10.1590/1678-9199-JVATITD-2020-0123.

Carone, S.E.I., Costa, T.R., Burin, S.M., Cintra, A.C.O., Zoccal, K.F., Bianchini, F.J., Tucci, L.F.F., Franco, J.J., Torqueti, M.R., Faccioli, L.H., Albuquerque, S., Castro, F. A., Sampaio, S.V., 2017. A new L-amino acid oxidase from *Bothrops jararacussu* snake venom: isolation, partial characterization, and assessment of pro-apoptotic and antiprotozoal activities. Int. J. Biol. Macromol. 103, 25–35. https://doi.org/10.1016/j.ijbiomac.2017.05.025.

Cheung, G.Y.C., Bae, J.S., Otto, M., 2021. Pathogenicity and virulence of *Staphylococcus aureus*. Virulence 12 (1), 547–569. https://doi.org/10.1080/21505594.2021.1878688.

CLSI (Clinical and Laboratory Standards Institute), 2012. M07-A9: methods for dilution antimicrobial susceptibility tests for bacteria that grow aerobically; approved standard, 9 end ed. Pennsylvanian 32 (2).

Colovos, C., Yeates, T.O., 1993. Verification of protein structures: patterns of nonbonded atomic interactions. Protein Sci. 2 (9), 1511–1519. https://doi.org/10.1002/pro.5560020916.

Costa, T.R., Menaldo, D.L., Oliveira, C.Z., Santos-Filho, N.A., Teixeira, S.S., Nomizo, A., Fuly, A.L., Monteiro, M.C., de Souza, B.M., Palma, M.S., St´abeli, R.G., Sampaio, S.V., Soares, A.M., 2008. Myotoxic phospholipases A(2) isolated from *Bothrops brazili* snake venom and synthetic peptides derived from their C-terminal region: cytotoxic effect on microorganism and tumor cells. Peptides (10), 1645–1656. https://doi.org/10.1016/j.peptides.2008.05.021.

Costa, T.R., Menaldo, D.L., Prinholato da Silva, C., Sorrechia, R., de Albuquerque, S., Pietro, R.C., Ghisla, S., Antunes, L.M., Sampaio, S.V., 2015. Evaluating the microbicidal, antiparasitic and antitumor effects of CR-LAAO from *Calloselasma rhodostoma* venom. Int. J. Biol. Macromol. 80, 489–497. https://doi.org/10.1016/j.ijbiomac.2015.07.004.

Costa, T.R., Carone, S.E.I., Tucci, L.F.F., Menaldo, D.L., Rosa-Garzon, N.G., Cabral, H., Sampaio, S.V., 2018. Kinetic investigations and stability studies of two *Bothrops* Lamino acid oxidases. J. Venom. Anim. Toxins Incl. Trop. Dis. 24, 37. https://doi.org/10.1186/s40409-018-0172-9.

de Melo Fernandes, T.A., Teixeira, S.C., Costa, T.R., Rosini, A.M., de Souza, G., Polloni, L., Barbosa, B.F., Silva, M.J.B., Ferro, E.A.V., Ávila, V.M.R., 2023. BjussuLAAO-II, an L-amino acid oxidase from *Bothrops jararacussu* snake venom, impairs *Toxoplasma gondii* infection in human trophoblast cells and villous explants from the third trimester of pregnancy. Microb. Infect. 25 (6), 105123 https://doi.org/10.1016/j.micinf.2023.105123.

Derby, C.D., Gilbert, E.S., Tai, P.C., 2018. Molecules and mechanisms underlying the antimicrobial activity of escapin, an L-amino acid oxidase from the ink of sea hares. Biol. Bull. 235 (1), 52–61. https://doi.org/10.1086/699175.

Fischetti, V.A., 2019. Surface proteins on gram-positive bacteria. Microbiol. Spectr. 7 (4) https://doi.org/10.1128/microbiolspec.GPP3-0012-2018, 10.1128/microbiolspec.GPP3-0012-2018.

Published in : Toxicon (2024), vol. 238, 107569
DOI: https://doi.org/10.1016/j.toxicon.2023.107569
Status : Postprint (Author's version)

Han, Y., Ma, B., Zhang, K., 2005. SPIDER: software for protein identification from sequence tags with de novo sequencing error. J. Bioinf. Comput. Biol. 3 (3), 697–716. https://doi.org/10.1142/s0219720005001247.

J Del Pozo, J.L., 2018. Biofilm-related disease. Expert Rev. Anti Infect. Ther. 16 (1), 51–65. https://doi.org/10.1080/14787210.2018.1417036.

Kasai, K., Nakano, M., Ohishi, M., Nakamura, T., Miura, T., 2021. Antimicrobial properties of L-amino acid oxidase: biochemical features and biomedical applications. Appl. Microbiol. Biotechnol. 105 (12), 4819–4832. https://doi.org/10.1007/s00253-021-11381-0.

Kwiecinski, J.M., Horswill, A.R., 2020. *Staphylococcus aureus* bloodstream infections: pathogenesis and regulatory mechanisms. Curr. Opin. Microbiol. 53, 51–60. https://doi.org/10.1016/j.mib.2020.02.005.

Laemmli, U.K., 1970. Cleavage of structural proteins during the assembly of the head of bacteriophage T4. Nature 227 (5259), 680–685. https://doi.org/10.1038/227680a0.

Laskowisck, R.A., MacArthur, M.W., Moss, D.S., Thornton, J.N., 1983. PROCHECK: a program to check the stereochemical quality of protein structures. J. Appl. Crystallogr. 26, 283–291. https://doi.org/10.1107/S0021889892009944.

Lazo, F., Vivas-Ruiz, D.E., Sandoval, G.A., Rodríguez, E.F., Kozlova, E.E.G., Costal-Oliveira, F., Chávez-Olórtegui, C., Severino, R., Yarlequé, A., Sanchez, E.F., 2017. Biochemical, biological and molecular characterization of an L-amino acid oxidase (LAAO) purified from *Bothrops pictus* Peruvian snake venom. Toxicon 139, 74–86. https://doi.org/10.1016/j.toxicon.2017.10.001.

Lee, M.L., Tan, N.H., Fung, S.Y., Sekaran, S.D., 2011. Antibacterial action of a heat-stable form of L-amino acid oxidase isolated from king cobra (*Ophiophagus hannah*) venom. Comp. Biochem. Physiol. C Toxicol. Pharmacol. 153 (2), 237–242. https://doi.org/10.1016/j.cbpc.2010.11.001.

Lüthy, R., Ju, Bowie, Eisenberg, D., 1992. Assessment of protein models with threedimensional profiles. Nature 356 (6364), 83–85. https://doi.org/10.1038/356083a0.

Ma, B., Zhang, K., Hendrie, C., Liang, C., Li, M., Doherty-Kirby, A., Lajoie, G., 2003. PEAKS: powerful software for peptide de novo sequencing by tandem mass spectrometry. Rapid Commun. Mass Spectrom. 17 (20), 2337–2342. https://doi.org/10.1002/rcm.1196.

Machado, A.R.T., Aissa, A.F., Ribeiro, D.L., Hernandes, L.C., Machado, C.S., Bianchi, M.L. P., Sampaio, S.V., Antunes, L.M.G., 2018. The toxin BjussuLAAO-II induces oxidative stress and DNA damage, upregulates the inflammatory cytokine genes TNF and IL6, and downregulates the apoptotic-related genes BAX, BCL2 and RELA in human Caco-2 cells. Int. J. Biol. Macromol. 109, 212–219. https://doi.org/10.1016/j.ijbiomac.2017.12.015.

Machado, A.R.T., Aissa, A.F., Ribeiro, D.L., Ferreira Jr., R.S., Sampaio, S.V., Antunes, L.M.G., 2019a. BjussuLAAO-II induces cytotoxicity and alters DNA methylation of cellcycle genes in monocultured/co-cultured HepG2 cells. J. Venom. Anim. Toxins Incl. Trop. Dis. 25, e147618 https://doi.org/10.1590/1678-9199-JVATITD-1476-18.

Published in : Toxicon (2024), vol. 238, 107569
DOI: https://doi.org/10.1016/j.toxicon.2023.107569
Status : Postprint (Author's version)

Machado, A.R.T., Aissa, A.F., Ribeiro, D.L., Costa, T.R., Ferreira Jr., R.S., Sampaio, S.V., Antunes, L.M.G., 2019b. Cytotoxic, genotoxic, and oxidative stress-inducing effect of an L-amino acid oxidase isolated from *Bothrops jararacussu* venom in a co-culture model of HepG2 and HUVEC cells. Int. J. Biol. Macromol. 127, 425–432. https://doi.org/10.1016/j.ijbiomac.2019.01.059.

Melo, R.T., Mendonça, E.P., Monteiro, G.P., Siqueira, M.C., Pereira, C.B., Peres, P.A.B.M., Fernandez, H., Rossi, D.A., 2017. Intrinsic and extrinsic aspects on *Campylobacter jejuni* biofilms. Front. Microbiol. 8, 1332. https://doi.org/10.3389/fmicb.2017.01332.

Nourbakhsh, F., Nasrollahzadeh, M.S., Tajani, A.S., Soheili, V., Hadizadeh, F., 2022. Bacterial biofilms and their resistance mechanisms: a brief look at treatment with natural agents. Folia Microbiol. 67 (4), 535–554. https://doi.org/10.1007/s12223-022-00955-8.

Oguiura, N., Sanches, L., Duarte, P.V., Sulca-López, M.A., Machini, M.T., 2023a. Past, present, and future of naturally occurring antimicrobials related to snake venoms. Animals 13 (4), 744. https://doi.org/10.3390/ani13040744.

Oguiura, N., Sanches, L., Duarte, P.V., Sulca-López, M.A., Machini, M.T., 2023b. Past, present, and future of naturally occurring antimicrobials related to snake venoms. Animals 13 (4), 744. https://doi.org/10.3390/ani13040744.

Okubo, B.M., Silva, O.N., Migliolo, L., Gomes, D.G., Porto, W.F., Batista, C.L., Ramos, C.S., Holanda, H.H., Dias, S.C., Franco, O.L., Moreno, S.E., 2012. Evaluation of an antimicrobial L-amino acid oxidase and peptide derivatives from *Bothropoides mattogrosensis* pitviper venom. PLoS One 7 (3), e33639. https://doi.org/10.1371/journal.pone.0033639.

Oliveira, A.L., Viegas, M.F., da Silva, S.L., Soares, A.M., Ramos, M.J., Fernandes, P.A., 2022. The chemistry of snake venom and its medicinal potential. Nat. Rev. Chem 6 (7), 451–469. https://doi.org/10.1038/s41570-022-00393-7.

Paloschi, M.V., Pontes, A.S., Soares, A.M., Zuliani, J.P., 2018. An update on potential molecular mechanisms underlying the actions of snake venom L-amino acid oxidases (LAAOs). Curr. Med. Chem. 25 (21), 2520–2530. https://doi.org/10.2174/0929867324666171109114125.

Peña-Carrillo, M.S., Pinos-Tamayo, E.A., Mendes, B., Domínguez-Borbor, C., Proaño-Bolaños, C., Miguel, D.C., Almeida, J.R., 2021. Dissection of phospholipases A2 reveals multifaceted peptides targeting cancer cells, *Leishmania* and bacteria. Bioorg. Chem. 114, 105041 https://doi.org/10.1016/j.bioorg.2021.105041.

Pereira-Crott, L.S., Casare-Ogasawara, T.M., Ambrosio, L., Chaim, L.F.P., de Morais, F.R., Cintra, A.C.O., Canicoba, N.C., Tucci, L.F.F., Torqueti, M.R., Sampaio, S.V., Marzocchi-Machado, C.M., Castro, F.A., 2020. *Bothrops moojeni* venom and BmooLAAO-I downmodulate CXCL8/IL-8 and CCL2/MCP-1 production and oxidative burst response, and upregulate CD11b expression in human neutrophils. Int. Immunopharm. 80, 106154 https://doi.org/10.1016/j.intimp.2019.106154.

Polloni, L., Costa, T.R., Morais, L.P., Borges, B.C., Teixeira, S.C., de Melo Fernandes, T.A., Correia, L.I.V., Bastos, L.M., Amorim, F.G., Quinton, L., Soares, A.M., Silva, M.J.B., Ferro, E.A.V., Lopes, D.S., de Melo Rodrigues Ávila, V., 2023. Oxidative stress induced by Pollonein-LAAO, a new L-amino

Published in : Toxicon (2024), vol. 238, 107569
DOI: https://doi.org/10.1016/j.toxicon.2023.107569
Status : Postprint (Author's version)

acid oxidase from *Bothrops moojeni* venom, prompts prostate tumor spheroid cell death and impairs the cellular invasion process in vitro. Cell. Signal. 109, 110785 https://doi.org/10.1016/j.cellsig.2023.110785.

Rabin, N., Zheng, Y., Opoku-Temeng, C., Du, Y., Bonsu, E., Sintim, H.O., 2015. Biofilm formation mechanisms and targets for developing antibiofilm agents. Future Med. Chem. 7 (4), 493–512. https://doi.org/10.4155/fmc.15.6.

Rey-Suárez, P., Acosta, C., Torres, U., Saldarriaga-Córdoba, M., Lomonte, B., Núñez, V., 2018. MipLAAO, a new L-amino acid oxidase from the redtail coral snake *Micrurus mipartitus*. PeerJ 6, e4924. https://doi.org/10.7717/peerj.4924.

Ruhal, R., Kataria, R., 2021. Biofilm patterns in gram-positive and gram-negative bacteria. Microbiol. Res. 251, 126829 https://doi.org/10.1016/j.micres.2021.126829.

Santos-Filho, N.A., Lorenzon, E.N., Ramos, M.A., Santos, C.T., Piccoli, J.P., Bauab, T.M., Fusco-Almeida, A.M., Cilli, E.M., 2015. Synthesis and characterization of an antibacterial and non-toxic dimeric peptide derived from the C-terminal region of Bothropstoxin-I. Toxicon 103, 160–168. https://doi.org/10.1016/j.toxicon.2015.07.004.

Sievers, F., Higgins, D.G., 2018. Clustal Omega for making accurate alignments of many protein sequences. Protein Sci. 27 (1), 135–145. https://doi.org/10.1002/pro.3290.

Singh, A., Amod, A., Pandey, P., Bose, P., Pingali, M.S., Shivalkar, S., Varadwaj, P.K., Sahoo, A.K., Samanta, S.K., 2022. Bacterial biofilm infections, their resistance to antibiotics therapy and current treatment strategies. Biomed. Mater. (2), 17. https://doi.org/10.1088/1748-605X/ac50f6.

Singkham-In, U., Thaveekarn, W., Noiphrom, J., Khow, O., Ponwaranon, S., Issara-Amphorn, J., Sitprija, V., Leelahavanichkul, A., 2023. Hydrogen peroxide from Lamino acid oxidase of king cobra (*Ophiophagus hannah*) venom attenuates Pseudomonas biofilms. Sci. Rep. 13 (1), 11304 https://doi.org/10.1038/s41598-023-37914-3.

Stábeli, R.G., Sant'Ana, C.D., Ribeiro, P.H., Costa, T.R., Ticli, F.K., Pires, M.G., Nomizo, A., Albuquerque, S., Malta-Neto, N.R., Marins, M., Sampaio, S.V., Soares, A. M., 2007. Cytotoxic L-amino acid oxidase from *Bothrops moojeni*: biochemical and functional characterization. Int. J. Biol. Macromol. 41 (2), 132–140. https://doi.org/10.1016/j.ijbiomac.2007.01.006.

Studer, G., Rempfer, C., Waterhouse, A.M., Gumienny, R., Haas, J., Schwede, T., 2020. QMEANDisCo-distance constraints applied on model quality estimation. Bioinformatics 36 (6), 1765–1771. https://doi.org/10.1093/bioinformatics/btz828.

Tong, H., Chen, W., Shi, W., Qi, F., Dong, X., So-Laao, 2008. A novel L-amino acid oxidase that enables *Streptococcus oligofermentans* to outcompete *Streptococcus mutans* by generating H_2O_2 from peptone. J. Bacteriol. 190 (13), 4716–4721. https://doi.org/10.1128/JB.00363-08.

Torrent, M., Di Tommaso, P., Pulido, D., Nogués, M.V., Notredame, C., Boix, E., Andreu, D., 2012. AMPA: an automated web server for prediction of protein antimicrobial regions. Bioinformatics 28 (1), 130–131. https://doi.org/10.1093/bioinformatics/btr604.

Published in : Toxicon (2024), vol. 238, 107569
DOI: https://doi.org/10.1016/j.toxicon.2023.107569
Status : Postprint (Author's version)

Toyama, M.H., Toyama Dde, O., Passero, L.F., Laurenti, M.D., Corbett, C.E., Tomokane, T.Y., Fonseca, F.V., Antunes, E., Joazeiro, P.P., Beriam, L.O., Martins, M. A., Monteiro, H.S., Fonteles, M.C., 2006. Isolation of a new L-amino acid oxidase from *Crotalus durissus cascavella* venom. Toxicon 47 (1), 47–57. https://doi.org/10.1016/j.toxicon.2005.09.008.

Ullah, A., 2020. Structure-Function studies and mechanism of action of snake venom Lamino acid oxidases. Front. Pharmacol. 11, 110. https://doi.org/10.3389/fphar.2020.00110.

Vargas Muñoz, L.J., Estrada-Gomez, S., Núñez, V., Sanz, L., Calvete, J.J., 2014. Characterization and cDNA sequence of *Bothriechis schlegelii* L-amino acid oxidase with antibacterial activity. Int. J. Biol. Macromol. 69, 200–207. https://doi.org/10.1016/j.ijbiomac.2014.05.039.

Vatansever, F., de Melo, W.C., Avci, P., Vecchio, D., Sadasivam, M., Gupta, A., Chandran, R., Karimi, M., Parizotto, N.A., Yin, R., Tegos, G.P., Hamblin, M.R., 2013. Antimicrobial strategies centered around reactive oxygen species bactericidal antibiotics, photodynamic therapy, and beyond. FEMS Microbiol. Rev. 37 (6), 955–989. https://doi.org/10.1111/1574-6976.12026.

Waterhouse, A., Bertoni, M., Bienert, S., Studer, G., Tauriello, G., Gumienny, R., Heer, F. T., de Beer, T.A.P., Rempfer, C., Bordoli, L., Lepore, R., Schwede, T., 2018. SWISSMODEL: homology modelling of protein structures and complexes. Nucleic Acids Res. 46 (W1), W296–W303. https://doi.org/10.1093/nar/gky427.

Wiezel, G.A., Rustiguel, J.K., Morgenstern, D., Zoccal, K.F., Faccioli, L.H., Nonato, M.C., Ueberheide, B., Arantes, E.C., 2019. Insights into the structure, function and stability of bordonein-L, the first L-amino acid oxidase from *Crotalus durissus terrificus* snake venom. Biochimie 163, 33–49. https://doi.org/10.1016/j.biochi.2019.05.009.

Williams, C.J., Headd, J.J., Moriarty, N.W., Prisant, M.G., Videau, L.L., Deis, L.N., Verma, V., Keedy, D.A., Hintze, B.J., Chen, V.B., Jain, S., Lewis, S.M., Arendall 3rd, W.B., Snoeyink, J., Adams, P.D., Lovell, S.C., Richardson, J.S., Richardson, D.C., 2018. MolProbity: more and better reference data for improved all-atom structure validation. Protein Sci. 27 (1), 293–315. https://doi.org/10.1002/pro.3330.

Wilton, M., Charron-Mazenod, L., Moore, R., Lewenza, S., 2015. Extracellular DNA acidifies biofilms and induces aminoglycoside resistance in *Pseudomonas aeruginosa*. Antimicrob. Agents Chemother. 60 (1), 544–553. https://doi.org/10.1128/AAC.01650-15.

Zhang, H., Yang, Q., Sun, M., et al., 2004. Hydrogen peroxide produced by two amino acid oxidases mediates antibacterial actions. J. Microbiol. 42, 336–339.